Spectral broadening in continuous-wave intracavity Raman lasers

Gerald M. Bonner,[1,2] Jipeng Lin,[1,*] Alan J. Kemp,[2] Jiyang Wang,[3] Huaijin Zhang,[3] David J. Spence,[1] and Helen M. Pask[1]

[1]*MQ Photonics, Department of Physics and Astronomy, Macquarie University, Sydney, NSW 2109, Australia*
[2]*Institute of Photonics, University of Strathclyde, SUPA, 106 Rottenrow, Glasgow, G4 0NW, UK*
[3]*State Key Laboratory of Crystal Materials and Institute of Crystal Materials, Shandong University, Jinan 250100, China*
[*]*Jipeng.lin@mq.edu.au*

Abstract: Spectral broadening of the fundamental field in intracavity Raman lasers is investigated. The mechanism for the spectral broadening is discussed and the effect is compared in two lasers using Raman crystals with different Raman linewidths. The impact of the spectral broadening on the effective Raman gain is analyzed, and the use of etalons to limit the fundamental spectral width is explored. It was found that an improvement in output power could be obtained by using etalons to limit the fundamental spectrum to a single narrow peak.

OCIS codes: (140.3550) Lasers, Raman; (140.3580) Lasers, solid-state; (190.0190) Nonlinear optics.

References and links

1. H. M. Pask, P. Dekker, R. P. Mildren, D. J. Spence, and J. A. Piper, "Wavelength-versatile visible and UV sources based on crystalline Raman lasers," Progress in Quant. Electron. **32**, 121–158 (2008).
2. A. J. Lee, D. J. Spence, J. A. Piper, and H. M. Pask, "A wavelength-versatile, continuous-wave, self-Raman solid-state laser operating in the visible," Opt. Express **18**(19), 20013–20018 (2010).
3. A. Lee, H. M. Pask, and D. J. Spence, "Control of cascading in multiple-order Raman lasers," Opt. Lett. **37**(18), 3840–3842 (2012).
4. A. J. Lee, H. M. Pask, J. A. Piper, H. Zhang, and J. Wang, "An intracavity, frequency-doubled $BaWO_4$ Raman laser generating multi-watt continuous-wave, yellow emission," Opt. Express **18**(6), 5984–5992 (2010).
5. X. Li, A. J. Lee, Y. Huo, H. Zhang, J. Wang, J. A. Piper, H. M. Pask, and D. J. Spence, "Managing SRS competition in a miniature visible Nd:YVO_4/$BaWO_4$ Raman laser," Opt. Express **20**(17), 19305–19312 (2012).
6. P. Dekker, H. M. Pask, D. J. Spence, and J. A. Piper, "Continuous-wave, intracavity doubled, self-Raman laser operation in Nd:$GdVO_4$ at 586.5 nm," Opt. Express **15**(11), 7038–7046 (2007).
7. P. Dekker, H. M. Pask, and J. A. Piper, "All-solid-state 704 mW continuous-wave yellow source based on an intracavity, frequency-doubled crystalline Raman laser," Opt. Lett. **32**(9), 1114–1116 (2007).
8. L. Fan, Y. X. Fan, Y. H. Duan, Q. Wang, H. T. Wang, G. H. Jia, and C. Y. Tu, "Continuous-wave intracavity Raman laser at 1179.5 nm with $SrWO_4$ Raman crystal in diode-end-pumped Nd:YVO_4 laser," Appl. Phys. B-Lasers and Optics **94**(4), 553–557 (2009).
9. L. Fan, Y. X. Fan, and H. T. Wang, "A compact efficient continuous-wave self-frequency Raman laser with a composite YVO_4/Nd:YVO_4/ YVO_4 crystal," Appl. Phys. B **101**(3), 493–496 (2010).
10. L. Fan, Y. X. Fan, Y. Q. Li, H. J. Zhang, Q. Wang, J. Wang, and H. T. Wang, "High-efficiency continuous-wave Raman conversion with a $BaWO_4$ Raman crystal," Opt. Lett. **34**(11), 1687–1689 (2009).
11. V. A. Lisinetskii, A. S. Grabtchikov, A. A. Demidovich, V. N. Burakevich, V. A. Orlovich, and A. N. Titov, "Nd:KGW/KGW crystal: efficient medium for continuous-wave intracavity Raman generation," Appl. Phys. B-Lasers and Optics **88**(4), 499–501 (2007).
12. D. C. Parrotta, A. J. Kemp, M. D. Dawson, and J. E. Hastie, "Multiwatt, continuous-wave, tunable diamond Raman laser with intracavity frequency-doubling to the visible region," IEEE Selected Topics in Quant. Electron. **19**, # 1400108 (2013).
13. Y. Sato and T. Taira, "Temperature dependencies of stimulated emission cross section for Nd-doped solid-state laser materials," Opt. Mater. Express **2**(8), 1076–1087 (2012).
14. Y. Sato and T. Taira, "Comparative study on the spectroscopic properties of Nd:$GdVO_4$ and Nd:YVO_4 with hybrid process," IEEE Selected Topics in Journal of Quant. Electron. **11**, 613–620 (2005).
15. Y. Sato and T. Taira, "Spectroscopic properties of Neodymium-doped Yttrium Orthovanadate single crystals with high-resolution measurement," Jpn. J. Appl. Phys. **41**(1), 5999–6002 (2002).

#206216 - $15.00 USD Received 10 Feb 2014; revised 15 Mar 2014; accepted 16 Mar 2014; published 24 Mar 2014

16. U. Keller and T. H. Chiu, "Resonant passive mode-locked Nd:YLF laser," IEEE J. Quantum Electron. **28**(7), 1710–1721 (1992).
17. T. T. Basiev, A. A. Sobol, Y. K. Voronko, and P. G. Zverev, "Spontaneous Raman spectroscopy of tungstate and molybdate crystals for Raman lasers," Opt. Mater. **15**(3), 205–216 (2000).
18. T. T. Basiev, A. A. Sobol, P. G. Zverev, V. V. Osiko, and R. C. Powell, "Comparative spontaneous Raman spectroscopy of crystals for Raman lasers," Appl. Opt. **38**(3), 594–598 (1999).
19. G. M. Bonner, H. M. Pask, A. J. Lee, A. J. Kemp, J. Wang, H. Zhang, and T. Omatsu, "Measurement of thermal lensing in a CW $BaWO_4$ intracavity Raman laser," Opt. Express **20**(9), 9810–9818 (2012).
20. J. J. Zayhowski, "The effects of spatial hole burning and energy diffusion on the single-mode operation of standing-wave lasers," IEEE J. Quantum Electron. **26**(12), 2052–2057 (1990).
21. A. Penzkofer, A. Laubereau, and W. Kaiser, "High intensity Raman interactions," Progress in Quant. Electron. **6**, 55–140 (1982).
22. J. Eggleston and R. Byer, "Steady-state stimulated Raman scattering by a multimode laser," IEEE J. Quantum Electron. **16**(8), 850–853 (1980).
23. E. A. Stappaerts, H. Komine, and W. H. Long, Jr., "Gain enhancement in Raman amplifiers with broadband pumping," Opt. Lett. **5**(1), 4–6 (1980).
24. A. T. Georges, "Statistical theory of Raman amplification and spontaneous generation in dispersive media pumped with a broadband laser," Phys. Rev. A **39**(4), 1876–1886 (1989).
25. A. Z. Grasiuk and I. G. Zubarev, "High-power tunable IR Raman lasers," Appl. Phys. (Berl.) **17**(3), 211–232 (1978).

1. Introduction

Continuous-wave (CW) intracavity Raman lasers can be compact and convenient sources of radiation in regions of the spectrum that are difficult to reach with other laser sources [1].

Despite the physical simplicity of intracavity Raman lasers, the interactions between the various electromagnetic fields and the population inversion in the laser gain crystal are complex. A variety of spectral competition effects can arise in these systems, including undesired cascading to higher Stokes orders [2, 3], competition between different Raman shifts in the Raman crystal [4] or between a Raman shift in the laser gain crystal and that in the Raman crystal [5], and broadening of the spectrum of the fundamental laser emission due to the spectrally-varying loss induced by Stokes field. In this paper, this broadening of the fundamental field will be studied in detail.

Broadening of the fundamental spectrum has been observed in a number of intracavity Raman lasers. Dekker *et al*. [6] observed complex structure developing in the fundamental and Stokes spectra of their frequency-doubled Nd:$GdVO_4$ self-Raman laser, with a second fundamental peak at 1066 nm appearing at high powers. This was attributed to the SRS-induced loss for the main fundamental transition at 1063 nm permitting the orthogonal 1066 nm transition to reach threshold [6]. The same group also observed spectral broadening in a frequency-doubled Nd:$GdVO_4$/$KGd(WO_4)_2$ system [7], with the fundamental field reaching a bandwidth of approximately 1 nm. The authors noted that the spectrum was most stable when the SRS conversion process strongly depleted the circulating fundamental field. Fan *et al*. [8] noted that the fundamental bandwidth varied from 0.15 to 0.55 nm in their Nd:YVO_4/$SrWO_4$ Raman laser, while the Stokes bandwidth varied from 0.05 to 0.35 nm, although the authors did not explicitly state the pump powers at which these measurements were made. Some of the same researchers observed similar broadening in a YVO_4/Nd:YVO_4/YVO_4 Raman laser [9], with the fundamental spectrum broadening from 0.23 nm at the Raman threshold to 1.09 nm at maximum power, whilst the Stokes spectral width varied from 0.14 nm to 0.52 nm. The same group also observed spectral broadening in a Nd:YVO_4/$BaWO_4$ laser [10], in which the fundamental spectrum broadened from 0.2 nm at the Raman threshold to 1.05 nm at maximum pump power, whilst the Stokes spectrum broadened from 0.15 nm to 0.5 nm. Lisinetskii *et al*. [11] observed that the fundamental field in their Nd:$KGd(WO_4)_2$/$KGd(WO_4)_2$ laser broadened from 5 cm^{-1} to 24 cm^{-1} (0.6 nm to 2.7 nm) while in an intracavity VECSEL/diamond Raman laser, broadening and complex spectral structure were also observed [12]. However, despite these numerous observations of spectral broadening in intracavity Raman lasers, to the best of the authors' knowledge, no detailed

#206216 - $15.00 USD Received 10 Feb 2014; revised 15 Mar 2014; accepted 16 Mar 2014; published 24 Mar 2014

investigation of this phenomenon has been undertaken prior to the study reported in this paper, and here we provide important new insight for selection of Raman gain media.

In Section 2 of this paper, the physical mechanism of the spectral broadening process will be described. In Section 3, observations of the spectral broadening in a Raman laser based on $BaWO_4$ will be presented and compared to the broadening in a similar laser using $KGd(WO_4)_2$. The impact of the broadening on the effective Raman gain will be analyzed in Section 4 and the effect on laser performance of using etalons to limit the broadening will be investigated in Section 5.

2. Broadening mechanism

In an ideal homogenously broadened laser, the longitudinal mode of the fundamental field closest to line center reaches threshold first, and saturates the laser gain to clamp the population inversion at its threshold level, thereby preventing any other longitudinal mode from oscillating. In practice, additional longitudinal modes often do reach threshold, commonly due to spatial-hole-burning in standing-wave laser cavities.

In intracavity Raman lasers, above the Raman threshold the SRS process itself presents a spectrally-varying loss to the fundamental field, which can lead to potentially severe broadening of the fundamental spectrum. Consider an idealized Raman laser running on a single fundamental longitudinal mode of frequency ν_0 at the centre of the laser gain spectrum, and a single Stokes longitudinal mode. We can write the net gain coefficient for fundamental frequencies around ν_0 as

$$\alpha_{NET}(\nu_0 - \delta\nu) = \alpha_F(\nu_0 - \delta\nu) - \Gamma(\nu_0 - \delta\nu) - \gamma_F. \quad (1)$$

where $\alpha_F(\nu)$ is the fundamental laser gain spectrum, $\Gamma(\nu)$ is the spectral loss to the fundamental due to SRS, and γ_F is the passive cavity loss for the fundamental. For a laser running on a single Stokes mode, the loss to the fundamental $\Gamma(\nu)$ due to the Stokes mode has the same spectral shape as the spontaneous Raman spectrum.

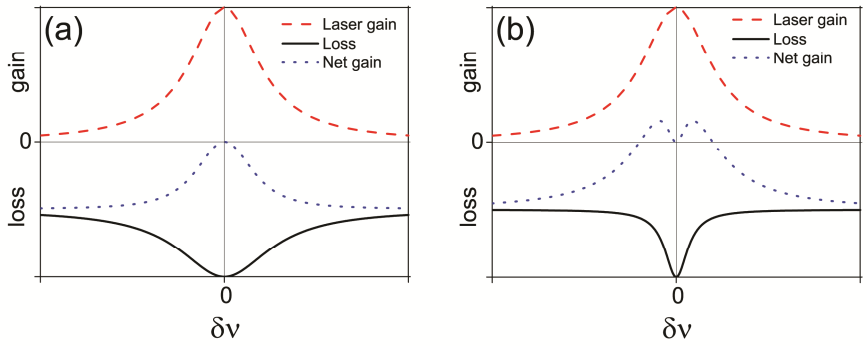

Fig. 1. Laser gain $\alpha_F(\nu_0 - \delta\nu)$ loss (including passive loss γ_F and loss due to the Stokes field $\Gamma(\nu_0 - \delta\nu)$), and net gain $\alpha_{NET}(\nu_0 - \delta\nu)$ for wavelengths around the fundamental frequency ν_0, for an idealized single-longitudinal mode laser pumped at two times the Raman pump power threshold. The laser gain and Raman spectrum are assumed to be Lorentzian, with widths $\Delta\nu_F$ and $\Delta\nu_R$ respectively. In (a) the Raman linewidth is wider than the laser linewidth with $\Delta\nu_R / \Delta\nu_F = 4/3$ and in (b) the Raman linewidth is narrower than the laser linewidth with $\Delta\nu_R / \Delta\nu_F = 1/3$.

#206216 - $15.00 USD Received 10 Feb 2014; revised 15 Mar 2014; accepted 16 Mar 2014; published 24 Mar 2014

Consider the case where the laser gain and Raman spectrum have the same lineshape. If the Raman linewidth $\Delta\nu_R$ is larger than the laser gain linewidth $\Delta\nu_F$, then $\alpha_{NET}(\nu_0) = 0$ will always have its peak value at $\delta\nu = 0$, and so our ideal single longitudinal mode Raman laser can operate stably. This is shown in Fig. 1(a), with $\alpha_{NET}(\nu_0) = 0$ and net loss for other fundamental modes.

However, if the Raman linewidth is smaller than the laser gain linewidth, then there will be a pump power for which $\alpha_{NET}(\nu)$ no longer takes its maximum value at $\delta\nu = 0$. This is shown in Fig. 1(b): in this situation the laser cannot operate stably on a single fundamental mode at ν_0, and the fundamental laser spectrum must broaden. This can lead to splitting of the fundamental field into two spectral peaks – indeed such splitting was reported in [6].

The broadening influence of the SRS process on the fundamental field thus depends on the relative sizes of the Raman linewidth and the laser gain linewidth. The Raman linewidths of several Raman crystals are given in Table 1, along with the gain bandwidths of several Nd-doped laser gain crystals. To avoid SRS-induced broadening of the fundamental, we would like $\Delta\nu_R >> \Delta\nu_F$. However, for most combinations of laser and Raman crystals, the Raman linewidth is smaller than the laser gain linewidth, and so we expect the SRS process to broaden the bandwidth of the laser radiation. For the present paper, we use Nd:YVO_4 as a laser material and $BaWO_4$ as a Raman material, and so with $\Delta\nu_R / \Delta\nu_F = 0.16$ we expect a relatively severe broadening effect, while a Nd:YVO_4/$KGd(WO_4)_2$ laser with $\Delta\nu_R / \Delta\nu_F = 0.66$ is also studied for comparison.

Table 1. Laser gain bandwidths and Raman linewidths for common laser and Raman crystals

	Wavelength/nm	Laser gain bandwidth/cm^{-1}
Nd:YAG	1064	5.3 [13]
Nd:$GdVO_4$	1063	8.8 [14]
Nd:YVO_4	1064	9.7 [15]
Nd:YLF	1047/1053	12 [16]
	Stokes shift/cm^{-1}	Raman linewidth/cm^{-1}
$BaWO_4$	925	1.6 [17]
Diamond	1333	2.7 [18]
$KGd(WO_4)_2$	901	5.4 [18]
$KGd(WO_4)_2$	768	6.4 [18]
$LiNbO_3$	872	21.4 [18]

3. Observations of spectral broadening

In this paper, the spectral behavior of a Nd:YVO_4/$BaWO_4$ intracavity Raman laser has been investigated in some detail. A $KGd(WO_4)_2$ Raman laser was also investigated for purposes of comparison. The spectra of the lasers were measured over a range of 1050 nm - 1190 nm using an Ocean Optics HR4000 spectrometer with a resolution of 0.09 nm and/or an Agilent 86142B Optical Spectrum Analyzer having a resolution of 0.06 nm. For each laser, the spectrum was recorded at various pump powers below and above the Raman threshold.

3.1 $BaWO_4$ Raman laser

The design of the $BaWO_4$ Raman laser is shown in Fig. 2. A disk geometry incorporating a diamond heat spreader was used for the Nd:YVO_4 laser gain material in order to reduce the thermal lens strength. Thermal lensing in the disk caused it to act like a concave mirror, which finite element analysis [19] predicted to have a radius of curvature of ~150 mm. The thermal lens was therefore sufficiently weak to permit a flexible cavity design, which facilitated the etalon experiments described later in this paper. A coupled cavity configuration was used to reduce the losses for the Stokes field, by excluding the laser gain disk from the

#206216 - $15.00 USD Received 10 Feb 2014; revised 15 Mar 2014; accepted 16 Mar 2014; published 24 Mar 2014

Stokes cavity, and to permit quasi-independent adjustment of the fundamental and Stokes cavities.

The laser was pumped with light at 808 nm from a fiber-coupled laser diode, focused to a spot of radius 300 μm in the Nd:YVO_4 disk, which was a 0.5 mm thick piece of a-cut Nd:YVO_4, having a doping concentration of 0.5 at.%. The disk was capillary bonded to a 0.75 mm thick piece of CVD diamond which served as an intracavity heatspreader. The pump beam was double passed through the disk, and a quarter waveplate was used to rotate the polarization of the unabsorbed pump light by 90° in between the passes so as to optimize the pump absorption. The Raman crystal was a 16 mm long piece of a-cut $BaWO_4$, grown at the State Key Laboratory of Crystal Materials, Shandong University. It was oriented so that the fundamental polarization was aligned perpendicular to its c-axis. The $BaWO_4$ crystal was AR-coated for the fundamental (1064 nm) and Stokes (1180 nm) wavelengths, while the intracavity diamond heatspreader was AR-coated for the fundamental wavelength. The crystals were mounted in water-cooled copper or brass mounts.

The fundamental resonator was defined by mirrors M1, M2 and M3. M1 was a coating on the back of the Nd:YVO_4 crystal, having high reflectivity (>99.9%) for the fundamental wavelength, while mirrors M2 and M3 were highly reflecting (>99.99%) at both fundamental and Stokes wavelengths, and had radii of curvature of 100 mm and −100 mm respectively. To enable better mode matching between fundamental and Stokes beams in the Raman crystal, a coupled Stokes resonator was employed. It was defined by mirrors M3, M2, DC and OC. Dichroic mirror DC was a plane mirror, highly transmitting (T>99.5%) at the fundamental wavelength of 1064 nm and highly reflecting (>99.9%) at the Stokes wavelength of 1180 nm. OC was a concave output coupler with a radius of curvature of 250 mm and a transmission of 0.4% at 1180 nm.

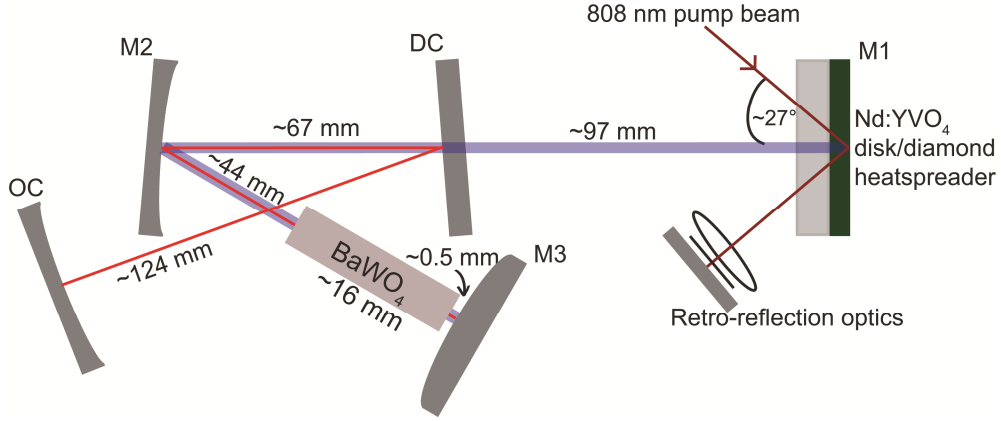

Fig. 2. Schematic of $BaWO_4$ laser cavity. DC was a plane dichroic mirror, highly transmitting at the fundamental wavelength of 1064 nm and highly reflecting at the Stokes wavelength of 1180 nm. M1 was a highly reflecting coating at the fundamental wavelength on the back of the Nd:YVO_4 crystal. M2 and M3 were highly reflecting at both wavelengths, and had radii of curvature of 100 mm and −100 mm respectively. OC was a concave output coupler with a radius of curvature of 250 mm and a transmission of 0.4% at 1180 nm.

The CW output power at the Stokes wavelength and the fundamental and Stokes spectra were measured simultaneously and are shown in Fig. 3 and Fig. 4 respectively. The fundamental and Stokes spectra have each been separately normalized to area over ranges of 10 nm, so that each trace represents the frequency spectrum of essentially the same number of fundamental or Stokes photons. Accordingly a decrease in the peak height can be interpreted as a general broadening of the spectrum. Note that the origins of the fundamental and Stokes plots are separated in wavenumber by the Stokes shift of $BaWO_4$ (925 cm^{-1}). Therefore

#206216 - $15.00 USD Received 10 Feb 2014; revised 15 Mar 2014; accepted 16 Mar 2014; published 24 Mar 2014

features in corresponding fundamental and Stokes plots which line up vertically are separated by the Stokes shift.

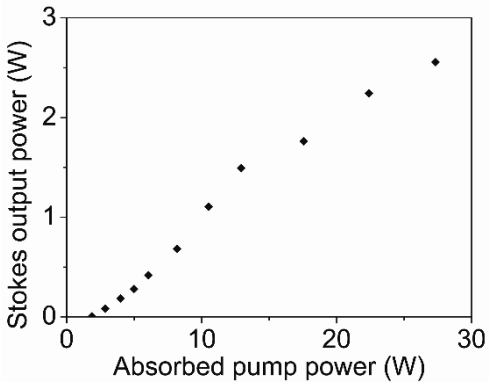

Fig. 3. Power transfer for the $BaWO_4$ Raman laser.

It can be seen from Fig. 4 that the fundamental spectrum broadens significantly as the pump power increases, from approximately 2.4 cm^{-1} (0.27 nm) below Raman threshold to 7.4 cm^{-1} (0.8 nm) at high pump powers. These spectral widths are similar to those observed by Fan *et. al.* in another Nd:YVO_4/$BaWO_4$ Raman laser [10]. Spectra were also collected with the Stokes cavity blocked, such that no SRS occurred and the fundamental field oscillated in a high Q cavity, and it was found that some broadening did occur, up to a maximum of 5 cm^{-1}, but not as much as when the Stokes field is oscillating. This non-SRS-induced broadening is likely to be due to spatial hole burning [20].

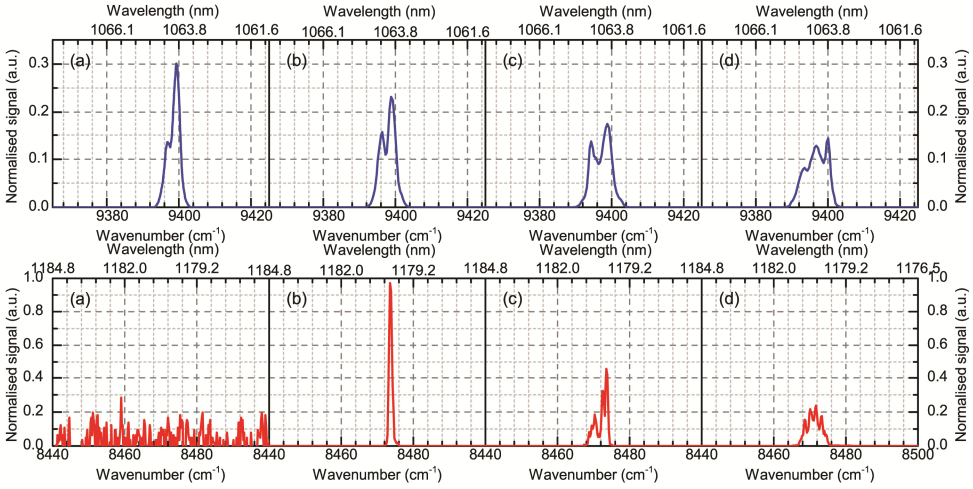

Fig. 4. Spectra of the $BaWO_4$ Raman laser. The upper plots (blue) show the fundamental spectra. The lower plots (red) show the corresponding Stokes spectra. The absorbed pump power was (a) 1.6 W (below Raman threshold), (b) 8.2 W, (c) 14.2 W, (d) 31.5 W.

3.2 $KGd(WO_4)_2$ Raman laser

For the purpose of comparison, we also investigated a $KGd(WO_4)_2$ Raman laser. Its design was very similar to that of the $BaWO_4$ Raman laser, except that due to the breakage of the crystal presented in the previous section, to the laser medium was a 1 at.% Nd:YVO_4 crystal that was bonded to a 0.5 mm thick diamond heatspreader. Both crystals provided almost identical lasing behavior in terms of the output power and spectral characteristics. The cavity length was adjusted to compensate for the different refractive indices and lengths of the

#206216 - $15.00 USD Received 10 Feb 2014; revised 15 Mar 2014; accepted 16 Mar 2014; published 24 Mar 2014

$BaWO_4$ and $KGd(WO_4)_2$ crystals. The 25 mm long KGW crystal was oriented so as to access the 768 cm^{-1} Raman shift, and a maximum output power of 2.6 W at 1158 nm was obtained.

Spectral broadening of the fundamental was much less significant in the $KGd(WO_4)_2$ Raman laser than in the $BaWO_4$ system, as shown in Fig. 5. (Note the appearance of a small feature at 9377cm^{-1} (1066nm) which is a secondary transition of Nd:YVO_4.) The broadest fundamental linewidth was 5 cm^{-1}, considerably lower than the 7.4 cm^{-1} observed for $BaWO_4$, and identical to that observed when SRS was suppressed by blocking the Stokes cavity. These observations are as expected, since the Raman linewidth of $KGd(WO_4)_2$ is greater than that of $BaWO_4$ but still less than the gain bandwidth of Nd:YVO_4. The broader Raman line of $KGd(WO_4)_2$ presents a broader loss to the fundamental field, reducing the propensity for broadening of the fundamental spectrum.

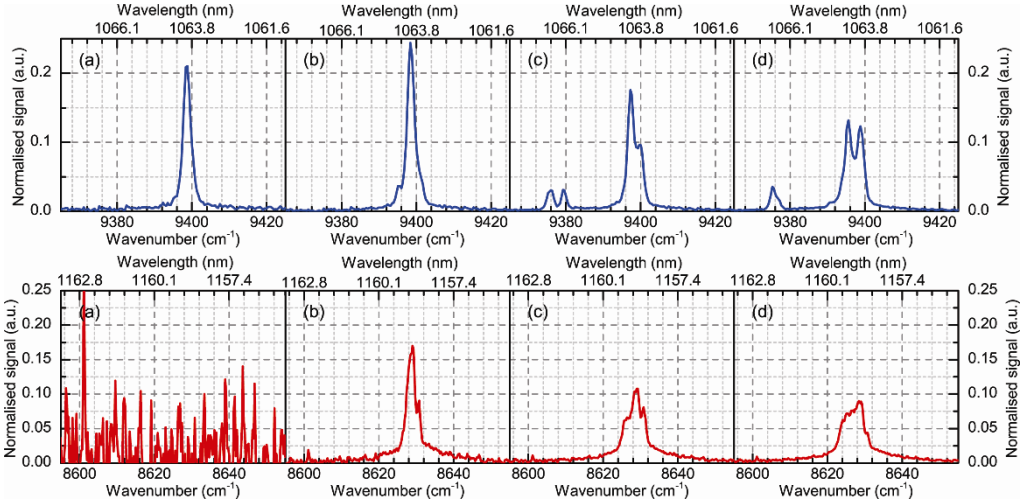

Fig. 5. Spectra of the $KGd(WO_4)_2$ Raman laser. Upper plots (blue) show the fundamental spectra. The lower plots (red) show the corresponding Stokes spectra. The absorbed pump power was (a) 0.90 W (below Raman threshold), (b) 3.98 W, (c) 12.94 W, (d) 27.33 W.

4. Impact of broadening on the effective Raman gain

Next we analyze the consequences of spectral broadening on the behavior of these lasers, in particular on the power flow between the fundamental and Stokes optical fields.

A material's Raman gain coefficient, g_R, is measured in "steady state", ideally using single-longitudinal mode CW pump lasers. For transform-limited pulses, the pulse duration of the fields relative to the dephasing time of the Raman material (or equivalently the linewidth of the laser fields compared to the linewidth of the spontaneous Raman spectrum) determines whether the SRS process is 'steady-state' or 'transient' [21] with the gain decreasing for pulses of fixed peak intensity as one moves from the steady state to the transient case.

For pulses that are not transform limited and for multi-longitudinal mode CW fields, the situation is far more complex, and depends on the properties of the Raman medium as well as on whether there are correlations between the fundamental and Stokes spectra. In the absence of strong dispersion, the full steady-state value of Raman gain can be maintained even if the fundamental laser linewidth is much broader than the Raman linewidth. This occurs because the Stokes and fundamental fields become correlated so that the phase difference between them is conserved for many times the coherence time of the individual fields. This can only occur in the absence of dispersion that would destroy the correlation. Several authors (e.g [22–24].) have calculated the critical intensity above which the Raman gain will become independent of the fields' linewidths, provided the fields copropagate for a sufficient distance for correlations to become established. It can be shown that for most gaseous Raman lasers

#206216 - $15.00 USD Received 10 Feb 2014; revised 15 Mar 2014; accepted 16 Mar 2014; published 24 Mar 2014

and for some pulsed crystalline lasers, the fundamental intensity will be above this critical value, and we must consider the effect of possible correlations.

For CW crystalline lasers, however, the round trips gains are much lower, and so we are not in the regime where gain is independent of the fields' linewidths (we calculate for the present laser that we are two orders of magnitude below the critical intensity). In this regime, no correlations are developed between the Stokes and pump fields. As the fundamental field linewidth becomes broader than the Raman linewidth, the coherence time of the pump field becomes less than the Raman dephasing time, and the Raman gain decreases. In this strong dispersion regime, each fundamental longitudinal mode independently provides gain for a range of Stokes modes determined by the Raman lineshape, and the gain spectrum for the Stokes is thus the convolution of the fundamental field lineshape and the Raman lineshape. For Lorentzian lineshapes of width $\Delta\nu_F$ and $\Delta\nu_R$ respectively, the gain at the line center of the Stokes spectra is given by $g_R\Delta\nu_R/(\Delta\nu_R + \Delta\nu_F)$ [24, 25]. This gain is appropriate for a spectrally-narrow Stokes signal, but we must account for a broad Stokes linewidth in the present lasers. The overall gain for a broad Stokes field with Lorentzian linewidth $\Delta\nu_S$ is given by $g_R\Delta\nu_R/(\Delta\nu_R + \Delta\nu_F + \Delta\nu_S)$. The measured fundamental and Stokes lines reported here are far from Lorentzian, and a more general formula for arbitrary spectral lines is given by

$$g_{eff} = g_R \int [R(\nu) * F(\nu)] S(\nu) \, \mathrm{d}\nu. \tag{2}$$

where $R(\nu)$ is the Raman linewidth normalized to have a peak value of 1, and $F(\nu)$ and $S(\nu)$ are the fundamental and Stokes lineshapes normalized to have an area of 1. The term in brackets (the convolution of the Raman lineshape with the fundamental spectrum) is the gain available to the Stokes field as a function of frequency. By taking the overlap integral of this spectral gain with the Stokes spectrum, the effective Raman gain g_{eff}, is retrieved. Since the power flow between the fundamental and Stokes field is proportional to g_{eff}, we expect a reduction of the effective gain coefficient to reduce the overall efficiency of a Raman laser. Conversely, if we can control and minimize the fundamental and Stokes linewidth, we can expect to substantially increase the efficiency of the Raman laser. Equation (2) will be applied to the $BaWO_4$ Raman laser considered already, and to a $BaWO_4$ Raman laser with etalons for linewidth control, in the next section.

5. Use of etalons to control spectral broadening

5.1 Experimental demonstration

Since the broadening of the fundamental spectrum can significantly reduce the effective Raman gain, the use of etalons to limit the spectral broadening was investigated using the $BaWO_4$ Raman laser described above. Two uncoated YAG etalons were used, one 400 μm thick and one 50 μm thick. The etalons were placed in the fundamental cavity only, between the dichroic mirror and the Nd:YVO_4/diamond unit.

The fundamental and Stokes spectra of the laser without any etalons in the cavity are shown in Fig. 6(a), the spectra of the laser with a single 400 μm thick etalon are shown in Fig. 6(b), and finally the spectra of the laser with both the 400 μm and the 50 μm thick etalons are shown in Fig. 6(c). These spectra were measured for the laser running near maximum power. Fundamental spectra were measured using the Ocean Optics HR4000 spectrometer with a resolution of 0.09 nm, while the Stokes spectra were measured using the Agilent-86142B OSA with resolution 0.06 nm, as before. Note that the spectra in Fig. 6(c) are instrument-limited; the actual linewidths at full-width half maximum (FWHM) are likely to be narrower than the measured values of 0.11 nm and 0.09 nm for the fundamental and Stokes respectively

#206216 - $15.00 USD Received 10 Feb 2014; revised 15 Mar 2014; accepted 16 Mar 2014; published 24 Mar 2014

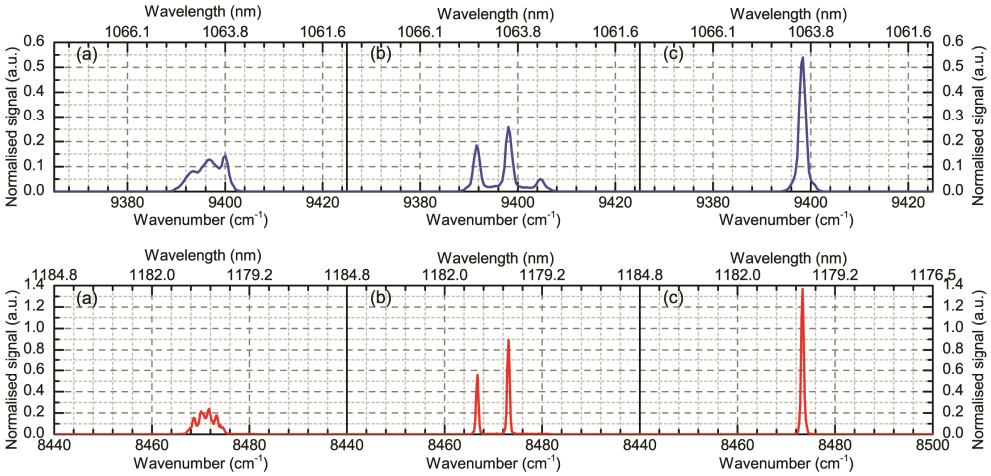

Fig. 6. Spectra of the $BaWO_4$ Raman laser with (a) no etalons, (b) the 400 μm thick YAG etalon and (c) both the 400 μm and the 50 μm thick etalons in the fundamental cavity The upper plots (blue) show the fundamental spectra when SRS is occurring. The lower plots (red) show the corresponding Stokes spectra. The absorbed pump power was 31.5 W. Note the instrument linewidths are 0.09 nm for the fundamental and 0.06 nm for the Stokes.

It can be seen that the 400 μm thick etalon is not effective in generating a single peak for fundamental spectrum. The free spectral range is 6.9 cm^{-1} (0.78 nm) and above threshold for SRS, the fundamental mode was found to oscillate at frequencies corresponding to neighboring transmission peaks of the etalon. When the 50 μm thick etalon is added, the broader free spectral range of 55.0 cm^{-1} (6.2 nm) is effective in suppressing the satellite peaks and a single narrow fundamental peak is obtained. Note that the 50 μm thick etalon used here is uncoated, and has broader transmission peaks than the 400 μm thick one, and therefore cannot be used on its own to suppress the spectral broadening. Ideally one would choose a 50 μm etalon with coatings to provide around 30% reflectivity at the fundamental wavelength, so that a single etalon can be used to provide the wide free spectral range and narrowband, potentially single longitudinal mode output.

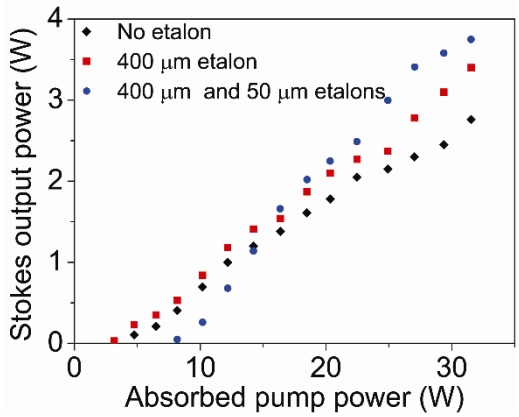

Fig. 7. Power transfers for the $BaWO_4$ Raman laser with and without etalons in the fundamental cavity.

Power transfers for the laser with and without the etalons are shown in Fig. 7. The 400 μm thick etalon alone leads to an increase in the maximum output power, while adding the 50 μm thick etalon leads to a further improvement. In particular, when both etalons are used, the

#206216 - $15.00 USD Received 10 Feb 2014; revised 15 Mar 2014; accepted 16 Mar 2014; published 24 Mar 2014

Raman threshold is higher, but the slope efficiency is also significantly higher, leading to a maximum output power of 3.75 W, compared to 2.76 W when no etalons are used. The overall efficiency when using the two etalons was 11.9% compared to 8.8% without etalons. It is also likely in this high-Q cavity that insertion losses (due to the imperfections in the surface finish and parallelism of the etalon perhaps) offset the benefits of linewidth control to some extent. A single, coated etalon of custom design would therefore be expected to improve the efficiency of this laser.

5.2 Calculation of effective Raman gain

We attribute the increase of efficiency of the laser with one and two added etalons to the decrease in the linewidth of the fields and thus the increase in the effective Raman gain. To confirm, the effective Raman gain was calculated using Eq. (2) using sets of spectral data for the three cases of no etalon, a single 400 μm etalon and the pair of 400 μm and 50 μm etalons and is plotted in Fig. 8 as a function of pump power.

It can be seen from Fig. 8 that the effective gain decreases as the fundamental spectrum broadens with increasing pump power when there are no etalons in the cavity. A similar trend is observed when the 400 μm etalon alone is used, due to energy leaking into the satellite peaks in the fundamental spectrum, which are not Raman-shifted so effectively. However, when both etalons are used together to maintain a single, narrow fundamental peak over the full range of pump powers investigated here, the effective gain is substantially higher. As noted above, the spectra measured for the case of using two etalons are instrument-limited, and the effective gain depicted in Fig. 8 is artificially suppressed, and is likely to be considerably higher. In the future, a Fabry-Pérot interferometer or similar instrument could be used to resolve the actual linewidth; however, such an instrument was not available when we undertook this study.

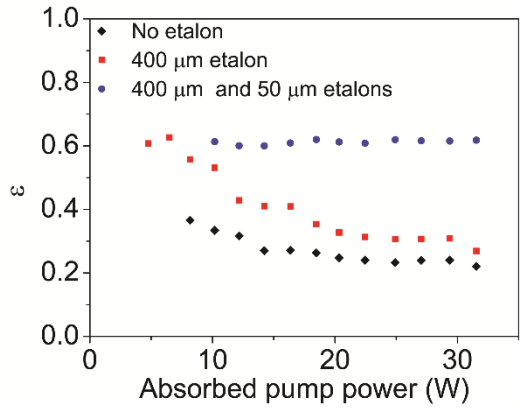

Fig. 8. The effective gain factor, $\varepsilon = g_{eff}/g_R$, calculated from the experimental spectral data for the Raman laser with and without etalons in the fundamental cavity.

It is clear from Fig. 8 that the spectral broadening in this intracavity $BaWO_4$ Raman laser can cause a substantial reduction in the effective Raman gain. By controlling the linewidth using etalons and increasing the effective Raman gain, we have achieved an increase in overall laser efficiency despite the additional insertion losses of the etalons. Note that for our narrowest measured linewidths, the effective gain factor is still only 0.6; using Eq. (2), we calculate that the fundamental and Stokes linewidths need to be <0.01 nm in order to access 90% of the peak Raman gain for $BaWO_4$.

#206216 - $15.00 USD Received 10 Feb 2014; revised 15 Mar 2014; accepted 16 Mar 2014; published 24 Mar 2014

6. Conclusion

Spectral broadening of the fundamental field in intracavity Raman lasers has been investigated theoretically and experimentally, and found to have a considerable impact on Raman laser performance through a reduction in the effective Raman gain. The extent to which spectral broadening occurs is dependent on the relative linewidths of the emission band of the laser gain crystal and the Raman transition of the Raman crystal. $\Delta\nu_R/\Delta\nu_F$ should be >1 if possible, with broadening becoming more severe as $\Delta\nu_R/\Delta\nu_F$ decreases between 1 and 0. Accordingly, these linewidths should be taken into account when designing an intracavity Raman laser for maximum efficiency. Indeed a crystal with lower Raman gain but a broader Raman bandwidth may be a superior choice if it maximizes the effective Raman gain when the finite linewidths of the intracavty fields are accounted for. In this paper where the laser gain crystal was Nd:YVO_4, severe spectral broadening was observed when $BaWO_4$, a Raman crystal with a narrow linewidth was used, while in a laser using $KGdWO_4$, the broadening was less significant. It has been shown that etalons can be used to limit the spectral broadening and in this way the output power and efficiency of the Raman laser can both be improved, if care is taken to minimize the insertion losses of the etalon(s).

Acknowledgments

G. M. Bonner received a DTA studentship from the EPSRC and an MQRES scholarship from Macquarie University. A. J. Kemp gratefully acknowledges funding from the EPSRC and the ERC.

#206216 - $15.00 USD Received 10 Feb 2014; revised 15 Mar 2014; accepted 16 Mar 2014; published 24 Mar 2014